

# Electroacupuncture Frequency-Related Transcriptional Response in Rat Arcuate Nucleus Revealed Region-Distinctive Changes in Response to Low- and High-Frequency Electroacupuncture

Ke Wang,<sup>1,3</sup> Rong Zhang,<sup>2</sup> Fei He,<sup>3</sup> Li-Bo Lin,<sup>3</sup> Xiao-Hui Xiang,<sup>2</sup> Xing-Jie Ping,<sup>2</sup> Ji-Sheng Han,<sup>2</sup> Guo-Ping Zhao,<sup>1,3</sup> Qing-Hua Zhang,<sup>1,3\*</sup> and Cai-Lian Cui<sup>2\*</sup>

<sup>1</sup>National Engineering Research Center for Biochip at Shanghai, Shanghai 201203, China

<sup>2</sup>Neuroscience Research Institute and Department of Neurobiology, Health Science Center, Key Laboratory of Neuroscience of the Ministry of Education and the Ministry of Public Health, Peking University, Beijing, 100191, China

<sup>3</sup>Shanghai—MOST Key Laboratory of Health and Disease Genomics, Chinese National Human Genome Center at Shanghai, Shanghai, 201203, China

Electroacupuncture (EA) has been clinically applied for treating different medical conditions, such as pain, strain, and immune diseases. Low- and high-frequency EAs have distinct therapeutic effects in clinical practice and experimental studies. However, the molecular mechanism of this difference remains obscure. The arcuate nucleus (Arc) is a critical region of the hypothalamus and is responsible for the effect of EA stimulation to remote acupoints. Gene expression profiling provides a powerful tool with which to explore the basis of physiopathological responses to external stimulus. In this study, using cDNA microarray, we investigated gene expressions in the rat Arc region induced by low-frequency (2-Hz) and high-frequency (100-Hz) EAs to two remote acupoints, zusanli (ST36) and sanyinjiao (SP6). We have found that more genes were differentially regulated by 2-Hz EA than 100-Hz EA (154 vs. 66 regulated genes/ESTs) in Arc, especially those related to neurogenesis, which was confirmed by qRT-PCR. These results demonstrate that the expression level of genes in the Arc region could be effectively regulated by low-frequency EA, compared with high-frequency EA, helping to uncover the mechanisms of the therapeutic effects of the low-frequency EA. Our results also indicate different-frequency EAs are spatially specific. © 2012 Wiley Periodicals, Inc.

**Key words:** electroacupuncture; transcriptional profile; arcuate nucleus

The clinical practice of acupuncture has become globally popular in recent years. It is believed that acupuncture stimulation to remote points is able to induce responses in certain brain regions to exert its functions.

In modern scientific research, zusanli (ST36) and sanyinjiao (SP6) are often used to study acupuncture effects on various physiological regulatory and control systems. It has been shown that stimulation to these two acupoints can modulate the neural functions and enhance the immune system to alleviate pain and improve neurological disorders (Hui et al., 2005; Han, 2011; Li et al., 2011; Wang et al., 2011). The effects have been thought to be mediated through changes in cellular activity, gene expression, and enzymatic activity in multiple remote tissues (Rho et al., 2008; Senna-Fernandes et al., 2009; Han, 2011). In addition, these acupoints in the rat are similar to those in humans in the sense of anatomy (Li et al., 2004).

Additional Supporting Information may be found in the online version of this article.

K. Wang and R. Zhang contributed equally to this work.

Contract grant sponsor: Chinese National Key Basic Research Project; Contract grant number: 973-2007CB512501; Contract grant sponsor: China Postdoctoral Science Foundation; Contract grant number: 20100480643.

\*Correspondence to: Qing-Hua Zhang, National Engineering Research Center for Biochip at Shanghai, 151 Libing Road, Shanghai 201203, People's Republic of China. E-mail: qinghua\_zhang@shbiochip.com or Cai-Lian Cui, Neuroscience Research Institute, Peking University, 38 Xueyuan Road, Beijing 100191, People's Republic of China. E-mail: clcui@bjmu.edu.cn.

Received 22 July 2011; Revised 7 December 2011; Accepted 16 December 2011

Published online 13 March 2012 in Wiley Online Library (wileyonlinelibrary.com). DOI: 10.1002/jnr.23028

Modern acupuncture, by giving precisely pulsed electrostimulations, has gradually been replacing traditional manual needling because of the accuracy in adjusting parameters and repeatability (Ulett et al., 1998; Zhao, 2008; Han, 2011). The frequency, intensity, and latency of EA significantly influence its therapeutic effects. Accumulating evidence suggests that low- and high-frequency EAs can be regarded as two distinct therapeutic methods and are disease-dependent in clinical practice (Wang et al., 2000; Zou et al., 2006; Y.S. Kim et al., 2008; Zhang et al., 2009). Studies have also shown that low- and high-frequency EA stimulations produced dissimilar therapeutic effects through different neurochemical mechanisms (Zhao, 2008; Han, 2011). For instance, low-frequency (2-Hz) EA accelerates the release of enkephalin,  $\beta$ -endorphin and endomorphin, whereas high-frequency (100-Hz) EA selectively increases dynorphin release in the central nervous system (CNS; Han, 2003). However, the molecular mechanisms underlying the different effects induced by the different frequencies of EAs are largely unknown.

The arcuate nucleus (Arc) region possesses a crucial site for nervous signal transduction and is also the key position for the nerve–endocrine–immune axis. The Arc of the hypothalamus is regarded as a synthesis site of opioid peptides ( $\beta$ -endorphinergic neurons), and the primary specific region in responding to low- instead of high-frequency EA (Han, 2003; Guo and Longhurst, 2007). It has been reported that low-frequency EA was able to increase Arc activity specifically to mediate analgesia and cardiovascular inhibition (Guo and Longhurst, 2007, 2010).

Gene expression profiles in the CNS can be used to decipher the molecular basis of specialized effect in detail (Robinson, 2004). Our previous study with cDNA microarray demonstrated that specific genes of certain gene ontology categories were spatiotemporally regulated and related to relevant molecular functions within specific CNS regions at the acute response stage (Wang et al., 2010). We hypothesized that identifying the differentially regulated genes in the Arc region induced by low- and high-frequency EAs could help in distinguishing the differences in their therapeutic effects. We stimulated ST36 and SP6 of rats with low- and high-frequency EAs (2 Hz and 100 Hz, respectively) and examined gene expressions in the Arc region with cDNA array to elucidate the molecular mechanisms underlying their different therapeutic effects.

## MATERIALS AND METHODS

### Animals

All experiments were performed on male Sprague-Dawley rats obtained from the Experimental Animal Center, Peking University, weighing 200–220 g at the beginning of the experiment. Animals were housed on a 12-hr light/dark cycle, with food and water available ad libitum. The room temperature was maintained at  $22^{\circ}\text{C} \pm 1^{\circ}\text{C}$  and relative humidity at 45–50%. Rats were handled daily during the first

3 days after arrival. All experimental procedures were approved by the Animal Care and Use Committee of Peking University Health Science Center.

### EA Stimulation

In total 32 male rats were used in the experiment. Eleven of them were given 2-Hz EA, another 11 were given 100-Hz EA, and the remaining 10 served as a control group without EA. EA stimulations were performed as described by Xing et al. (2007). In brief, stainless-steel needles 0.3 mm in diameter and 3 mm in length were bilaterally inserted in hind legs, one at the acupoint ST36 and the other at the acupoint SP6. Constant-current square-wave electrical stimulation generated by a programmed pulse generator (HANS, LH 800; manufactured by Peking University of Astronautics and Aeronautics Aviation) was given via the two needles for a total of 30 min. The frequency was set at either 2 Hz or 100 Hz. The intensity of stimulation was increased stepwise from 0.5 to 1.0 and then 1.5 mA, with each step lasting for 10 min.

### RNA Extraction and cDNA Microarray Hybridization

Rats were given an overdose of chloral hydrate (250 mg/kg, i.p.) after 1 hr of 2-Hz or 100-Hz EA stimulation and were decapitated immediately. Their brains were quickly removed and frozen in N-hexane ( $-70^{\circ}\text{C}$ ) for approximately 40 sec. The brain samples were then stored at  $-80^{\circ}\text{C}$  until further use. Arc and the remainder of the hypothalamus around the Arc punches were obtained from 60- $\mu\text{m}$ -thick sections taken on a sliding freezing microtome according to a stereotaxic atlas of the rat brain (Paxinos and Watson, 1998; Supp. Info. Fig. 1), stored immediately in cold RNAlater (Ambion, Austin, TX), and then stored at  $-80^{\circ}\text{C}$  until later experiments.

Total RNA was isolated using the Trizol reagent (Invitrogen, Carlsbad, CA) and purified with RNeasy column (Qiagen, Valencia, CA). The RNA concentration and purity were analyzed by a Nanodrop spectrophotometer (Nanodrop Technologies, Wilmington, DE), with the spectral absorption at 260 and 280 nm. The assessment of RNA integrity was conducted with an Agilent 2100 Bioanalyzer (Agilent Technologies, Palo Alto, CA). The cDNA microarray platform containing 11,444 rat genes/ESTs was submitted to the GEO database with the accession number GPL3498. Microarray manufacture, experimental procedures, and data extraction strategy were performed as previously described (Wang et al., 2010). Low RNA Input Fluorescent Linear Amplification Kit (Agilent Technologies) was used for RNA linear amplification following the manufacturer's protocol (Xie et al., 2009). For the microarray experiment, 2  $\mu\text{g}$  of each total RNA sample was used. Equal amounts of RNA from the Arc tissues of three control rats were pooled as a reference and labeled with Cy3. RNA samples from Arc of the 2-Hz group ( $n = 6$ ) and 100-Hz group ( $n = 6$ ) were individually labeled with Cy5. After hybridization, the slides were scanned using GenePix 4000B scanner (Axon Instruments, Foster City, CA), and the data were extracted with the GenePix Pro6.0 software package.

TABLE I. Sequences of Primers for qRT-PCR

Symbol	GenBank	Forward primer	Reverse primer
<i>CycA</i>	XM_345810	AGCACTGGGGAGAAAAGGATT	AGCCACTCAGTCTTGGCAGT
<i>Gapdh</i>	NM_017008	TCCTGCACCACCAACTGCTTAG	AGTGGCAGTGATGGCATGGACT
<i>Ywhaz</i>	BC094305	TTGAGCAGAAGACGGAAGGT	GAAGCATTGGGGATCAAGAA
<i>Dusp1</i>	NM_053769	TTCAAAGCCCCATCACAACC	TTGCATTGCTCCTCCCATG
<i>Fabp7</i>	NM_030832	GGTTGGATGGAGACAAGCTC	TAACAGCGAACAGCAACGAC
<i>Foxg1</i>	NM_012560	GAGGTGCAATGTGGGGAGAAAT	CTGCACACATGGAAAATCTGG
<i>Gria3</i>	NM_032990	AAGGCTCAGCATTAGGAACGC	CCCCTTATCGTACCACCATTGT
<i>Nr4a3</i>	NM_031628	TGCTTGCTCTGCACCATTTC	GCATGGGCAATCTGCTATTT
<i>Sgk1</i>	NM_019232	TGCAGTGACGAGCATCCAGAT	CAATGAAACACCAACGGCTCT

### Bioinformatics Analysis

Data normalization of each microarray was accomplished by intensity-dependent locally weighted scatterplot smoothing regression analysis (LOWESS) in the GeneSpring 6.1 software package (Agilent Technologies). The spots with low signal: noise ratio (<2) were automatically eliminated, and only those genes present in more than three samples (50%) in each group were used in further analysis. Principal components analysis (PCA) was employed to summarize gene expression profiles between groups. To compare the concentration and discreteness of 2-Hz and 100-Hz groups, we calculated the distances from the center of each group to the observed point for each subject in each group. Also, we applied homogeneity of variance tests between groups in the usual *t*-test setting. Partial least squares discriminative analysis (PLS-DA) was also used to test whether there were any difference between 2 Hz and 100 Hz. Regulated genes were identified by significance analysis of microarrays (SAM; Tusher et al., 2001), with a false discovery rate (FDR) <0.01 and average regulation of the gene no less than 1.4-fold against the control group.

Biological themes associated with differentially expressed genes were identified by Gene Ontology (GO) categories of biological process by the functional annotation tool of the Database for Annotation, Visualization, and Integrated Discovery (DAVID; <http://david.abcc.ncifcrf.gov/>; Huang et al., 2009). This procedure was used in order to identify the important GO categories (enrichment, EASE score  $\geq 1.0$ ) and to test their potential biological significance. The biological process of differently expressed genes could be ranked by the EASE score based on all enriched annotation terms.

To provide functional interpretation, regulated gene pathways were explored by the Kyoto Encyclopedia of Genes and Genomes (KEGG) online database (<http://www.genome.jp/kegg/>). The KEGG pathways of the differentially expressed genes were matched with the tool of DAVID Functional Annotation, which also gives a modified Fisher exact *P* value for pathway enrichment analysis.

### Quantitative RT-PCR

For cDNA synthesis, oligo(dT) primers, 1  $\mu$ g of each total RNA sample, and the Superscript II reverse transcriptase (Invitrogen) were used, following the guidelines of the manufacturer. cDNA samples were placed on ice and stored at  $-20^{\circ}\text{C}$  until further use. Prior to the analysis, 20  $\mu$ l of each cDNA sample was diluted with 180  $\mu$ l of MilliQ water. qPCRs were performed with the Prism 7900 Sequence Detection System

(Applied Biosystems). For each reaction, 1  $\mu$ l of each diluted cDNA sample was added to a mixture containing 12.5  $\mu$ l of  $2 \times$  SYBR green II qRT-PCR kit (Toyobo, Osaka, Japan), 1  $\mu$ l of each primer (5  $\mu\text{M}$ ), and 10.5  $\mu$ l of MilliQ water. The primer sequences are listed in Table I. Cycling conditions were 10 min  $95^{\circ}\text{C}$ , followed by 40 cycles of 15 sec at  $95^{\circ}\text{C}$  and 1 min at  $60^{\circ}\text{C}$ . After cycling, a melting protocol was performed with 15 sec at  $95^{\circ}\text{C}$ , 1 min at  $60^{\circ}\text{C}$ , and 15 sec at  $95^{\circ}\text{C}$ , to control for product specificity.

The glyceraldehyde-3-phosphate dehydrogenase gene (*Gapdh*) with stable expression in each sample in the microarray experiment and cyclophilin A (*CycA*) and tyrosine 3-monooxygenase/tryptophan (*Ywhaz*) genes, which are identified as the two most stably expressed housekeeping genes in the brain, were chosen as the potential endogenous control (Bonfeld et al., 2008). Thereafter, the endogenous control gene selected by the NormFinder program (Andersen et al., 2004) was used in subsequent qRT-PCR analysis. The fold change (FC) in target gene cDNA relative to selected endogenous control gene was determined as follows:  $\text{FC} = 2^{-\Delta\Delta\text{Ct}}$ , where  $\Delta\Delta\text{Ct} = (\text{Ct}_{\text{Target}} - \text{Ct}_{\text{Control}})_{\text{test}} - (\text{Ct}_{\text{Target}} - \text{Ct}_{\text{Control}})_{\text{control}}$ . Ct values were defined as the number of the PCR cycles at which the fluorescence signals were detected. To increase the reliability and integrity of the study results and to promote experimental consistency and transparency between research laboratories, a Minimum Information for Publication of Quantitative Real-Time PCR Experiments (MIQE) checklist is supplied as Supporting Information Table 1 according to the MIQE guidelines (Bustin et al., 2009). In qRT-PCR analysis, data are presented as mean  $\pm$  SEM and were analyzed with one-way analysis of variance (ANOVA) followed by the Tukey's HSD post hoc test in SPSS 13.0 (SPSS, Chicago, IL).

## RESULTS

### Transcriptional Modulation After Different Frequency EA

Gene expression profiles in the Arc region were measured after 2-Hz or 100-Hz EA stimulations. After filtering for high-quality array data (see Materials and Methods), the global transcriptional profiling with 7,885 genes/ESTs of the Arc region after 2-Hz and 100-Hz EA stimulations were displayed in PCA and PLS-DA plots. The PCA showed that the EA-stimulated rats in two groups were separated, indicating that there were no abundantly large transcriptional changes

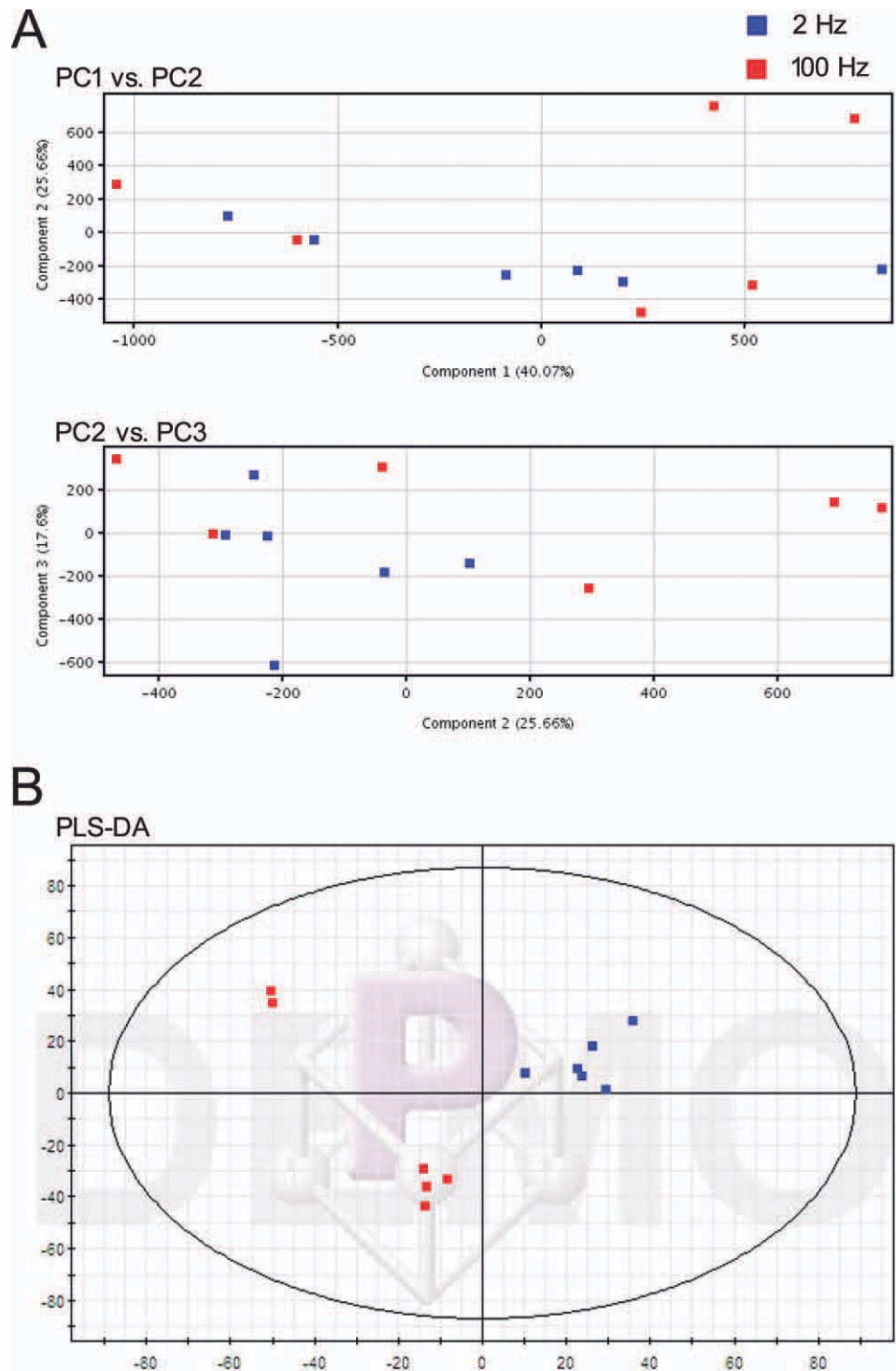


Fig. 1. Global analysis of results of transcriptome profile experiment of 2-Hz/100-Hz EA effects on Arc gene expression. **A:** PCA analysis of the filtered 7,885 genes/ESTs of all samples from all arrays in the Arc region induced by 2-Hz/100-Hz EA. **B:** PLS-DA analysis to test the differences between 2 Hz and 100 Hz. [Color figure can be viewed in the online issue, which is available at [wileyonlinelibrary.com](http://wileyonlinelibrary.com).]

in naïve rats (Fig. 1A). However, the 100-Hz EA-stimulated rats ( $n = 6$ ) were more separated from each other than 2-Hz EA-stimulated rats ( $n = 6$ ). In com-

paring the distance from each point to the center of the 2-Hz group with the 100-Hz group, there was a significant difference ( $P < 0.05$ ). The PLS-DA also



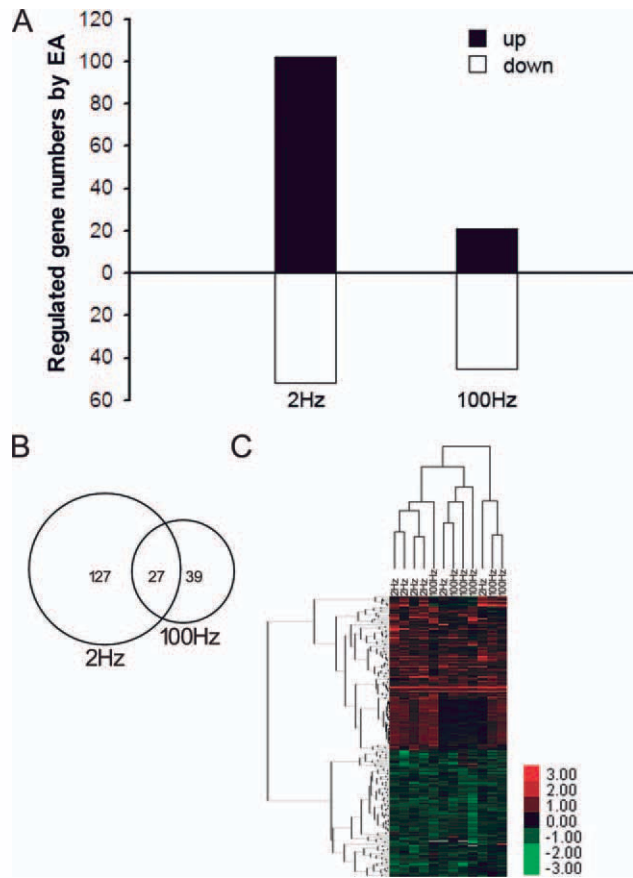


Fig. 2. Regulation of gene expression by 2-Hz and 100-Hz EA. **A:** Numbers of differentially expressed genes/ESTs in the Arc region after 2-Hz or 100-Hz EA stimulations. List of the complete regulated genes for each group is given in Supporting Information Tables 2 and 3. **B:** Overlapped and nonoverlapped regulated genes/ESTs induced by 2-Hz and 100-Hz EA. The diagram shows the number of genes/ESTs with the indicated expression patterns. **C:** Clustering display of differentially expressed genes/ESTs using the unsupervised hierarchical clustering method. Log<sub>2</sub> ratios were color coded as indicated. [Color figure can be viewed in the online issue, which is available at [wileyonlinelibrary.com](http://wileyonlinelibrary.com).]

showed a difference in the gene expression of 2-Hz and 100-Hz groups (Fig. 1B). By using the high-stringency analysis with SAM (Tusher et al., 2001) at FDR < 0.01, 536 genes/ESTs in the 2-Hz group and 78 genes/ESTs in the 100-Hz group were remained. Among these genes/ESTs, 154 and 66 were identified as differently regulated, with average regulation  $\geq 1.4$ -fold in 2-Hz and 100-Hz groups, respectively (Fig. 2A,B).

**2-Hz EA-regulated genes.** For the functional annotation of the differentially expressed genes, 102 up-regulated and 52 downregulated genes/ESTs labeled with Genebank ID were subjected to the DAVID Functional Annotation Tool to identify enrichment of potential biological processes (Huang et al., 2009). Genes were classified by using gene ontology (GO) terms (EASE score  $\geq 1$ ). Although no specific biological processes were enriched in the downregulated genes, seven processes were enriched in the upregulated genes (Table II), including embryonic organ morphogenesis (GO:0048562), positive regulation of ion transport (GO: 0043270), positive regulation of cell growth (GO:0030307), positive regulation of neurogenesis (GO:0050769), response to hormone stimulus (GO:0009725), microtubule cytoskeleton organization (GO:0000226), and positive regulation of transcription (GO:0045941). Most of the processes are related to neurogenesis. To understand better the higher order functional association of the differentially expressed genes, Kyoto Encyclopedia of Genes and Genomes (KEGG) pathway analysis was carried out with the application of the DAVID Annotation Tool. The long-term depression (LTD; rno04730) pathway was enriched in 2-Hz-induced genes ( $P < 0.05$ ; Table III).

**100-Hz EA-regulated genes.** For the 100-Hz EA-induced genes/ESTs, the 21 upregulated genes/ESTs labeled with Genebank ID were enriched in two categories, regulation of apoptosis (GO: 0042981) and phosphate metabolic process (GO: 0006796), and the 45 downregulated genes were enriched in two categories, regulation of hydrolase activity (GO: 0051336) and response to metal ion (GO: 0010038; Table II). With KEGG pathway

TABLE II. Enriched GO Categories Were in 2-Hz- and 100-Hz-Regulated Genes by DAVID Analysis

Group	Term	GO accession ID	Expression pattern (up/down)	Enrichment score	Gene name	
2 Hz	Embryonic organ morphogenesis	GO: 0048562	Up	1.68	<i>Gjb6, Nr4a3, Foxg1, Gnas</i>	
	Positive regulation of ion transport	GO: 0043270	Up	1.65	<i>Homer1, P2ry1, Sgk1</i>	
	Positive regulation of cell growth	GO: 0030307	Up	1.48	<i>Mapt, Sgk1, Alox15</i>	
	Positive regulation of neurogenesis	GO: 0050769	Up	1.29	<i>Mapt, Foxg1, Sgk1</i>	
	Response to hormone stimulus	GO: 0009725	Up	1.19	<i>Mb, Dusp1, Nr4a3, Gnas, Sgk1</i>	
	Microtubule cytoskeleton organization	GO: 0000226	Up	1.18	<i>Mapt, Pcm1, Sgk1</i>	
	Positive regulation of transcription	GO: 0045941	Up	1.11	<i>Plagl1, Klf4, Nr4a3, Zfp423, Nr4a1</i>	
	100 Hz	Regulation of apoptosis	GO: 0042981	Up	2.33	<i>Dusp1, Hspa1a, Nr4a1, Sgk1</i>
		Phosphate metabolic process	GO: 0006796	Up	1.35	<i>Gadd45g, Dusp1, Sgk1</i>
Regulation of hydrolase activity		GO: 0051336	Down	1.68	<i>Bad, Bax, Thy1, Ntsr2</i>	
Response to metal ion		GO: 0010038	Down	1.39	<i>Bad, Bax, Apbb1</i>	

analysis, the MAPK signaling pathway (rno04010) was enriched in 100-Hz group (Table III).

**Coregulated genes in response to EA.** To explore the common characteristics in Arc involved in EA response, the genes that were coregulated after 2-Hz/100-Hz EA stimulations were analyzed. Twenty-seven genes/ESTs were identified as being coregulated in response to EA stimulation in the Arc (Supp. Info. Table 4). Importantly, the expression of these coregulated genes were in the same directions (up- or down-), and there was a significant correlation between 2-Hz and 100-Hz EA (Pearson's correlation coefficient,  $R = 0.92$ ,  $P < 0.001$ ; Fig. 3, Supp. Info. Table 4). Among these coregulated (17 up- and 10 downregulated) genes/ESTs, only upregulated genes/ESTs were enriched in regulation of apoptosis (GO: 0042981; Table IV). Except for the coregulated genes, the remaining 127 and 39 genes/ESTs were in the 2-Hz and 100-Hz group, respectively (Fig. 2B). Hence, these regulated genes/ESTs might have correlations with frequencies. Based on this analysis, differentially regulated genes in 2-Hz EA were only enriched in embryonic organ morphogenesis (GO: 0048562) with upregulated genes, and 100-Hz frequency-related genes were enriched in regulation of hydrolase activity (GO: 0051336) with downregulated genes (Table IV).

### Validation of Microarray Array Results

First, the NormFinder software adopts a model-based approach and provides a ranking order according to expression stability. According to this program (Fig. 4), *CycA* was identified as the most stable gene and was selected as reference gene for gene expression normalization in the qRT-PCR experiment. To verify the results obtained by the cDNA microarray analysis, six differentially expressed genes of interest were chosen, and their expression levels were evaluated by qRT-PCR. Three genes (*Dusp1*, *Gria3*, and *Sgk1*) were involved in neurogenesis, which was more likely associated with 2-Hz and 100-Hz EA effects. The other three genes (*Fabp7*, *Foxg1*, and *Nr4a3*) were specially regulated by 2-Hz EA. Figure 5 showed that the expression profiles of the representative genes in qRT-PCR analysis corresponded to the microarray

ray results with SAM analysis. Table V displays the microarray and the qRT-PCR fold change results. Except for *Foxg1* in the 2-Hz group, there were no significant differences in the fold change values quantified according to the paired *t*-test. In summary, the microarray results were verified by the qRT-PCR analysis.

To determine whether these regulated genes were region-specifically changed in Arc, we have carried out an additional animal experiment with the same experimental manipulation (EA) as previous rats used for microarray. The Arc tissues and the remainder of the hypothalamus around the Arc were collected from these animals ( $n = 5$  per group; Supp. Info. Fig. 1). We carried out qRT-PCR to explore the gene expression regulations in the Arc region and the remaining-region tissues after EA stimulations. The genes that were previously selected for verifying the reliability of the microarray results were selected by qRT-PCR. As shown in Figure 6, five of them showed the same regulations in the Arc region but no significant regulated in the remaining tissues of the hypothalamus. Interestingly, the stress-related gene *Sgk1* had wide regulation in both the Arc and the remaining tissues.

### DISCUSSION

The frequency of EA is an important parameter in clinical treatment because of its influence on EA's therapeutic effects. Variable effects of EA therapy with different frequencies contribute to variable results (Zou et al., 2006; H.W. Kim et al., 2008; Y.S. Kim et al., 2008). The different frequencies of EA have unique therapeutic effects through activating different biological responses by transcriptional and nontranscriptional mechanisms (Zhao, 2008; Han, 2011). In this study, cDNA microarray was used to examine gene expression in the Arc region induced by 2-Hz/100-Hz EA stimulations.

The Arc of the hypothalamus, as a critical site for neurocircuits to mediate the effect of 2-Hz EA, regulates a number of pathophysiological processes, including emotion, autonomic activity, and pain, etc. (Liu et al., 2007; Cassaglia et al., 2011; Peng et al., 2011). Previous studies proved that the Arc region participates in the cardiovascular, endocrine, and analgesic effects of EA by applying neuropharmacology and neurochemistry methods in animal experiments (Zhao, 2008). This study showed a frequency-dependent variation of global gene expression changes in the Arc region with 2-Hz and 100-Hz EA stimulations. The PCA in this experiment showed that gene expression of the Arc induced by the 100-Hz EA stimulation was more separate than that

**TABLE III. Enriched KEGG Pathways Were in 2-Hz- and 100-Hz-Regulated Genes**

Group	Pathway name	KEGG ID	P value	Gene name
2 Hz	Long-term depression	rno04730	0.04	<i>Plcb1</i> , <i>Gria3</i> , <i>Gnas</i>
100 Hz	MAPK signaling pathway	rno04010	0.04	<i>Gadd45g</i> , <i>Dusp1</i> , <i>Hspa1a</i> , <i>Nr4a1</i>

**TABLE IV. Enriched GO Categories in EA-Related and Frequency-Related Genes**

Group	Term	GO accession ID	Expression pattern (up/down)	Enrichment score	Gene name
EA-related	Regulation of apoptosis	GO: 0042981	Up	2.04	<i>Dusp1</i> , <i>Nr4a1</i> , <i>Sgk1</i>
2-Hz-related	Embryonic organ morphogenesis	GO: 0048562	Up	1.98	<i>Gjb6</i> , <i>Nr4a3</i> , <i>Foxg1</i> , <i>Gnas</i>
100-Hz-related	Regulation of hydrolase activity	GO: 0051336	Down	2.03	<i>Bad</i> , <i>Bax</i> , <i>Thy1</i> , <i>Ntsr2</i>

induced by the 2-Hz EA stimulation (Fig. 1A). The PLS-DA demonstrated that the 2-Hz group and 100-Hz group were distinguishable in distribution. This showed that low- and high-frequency stimulation in the Arc region could induce significant differences in the gene expression (Fig. 1B). As shown in Figure 1, two samples deviated from the other four samples in the 100-Hz group. This deviation may be due mainly to the biological

variability, because there was no difference in technical variability such as RNA quality or yield. Furthermore, gene expression profiling revealed that there were greater changes and much more sensitivity and homogeneity in gene expression regulations with 2-Hz vs. 100-Hz EA stimulation (Fig. 2). Previous studies from our laboratory showed that the expression of c-Fos, as a marker of neuronal activities, was especially increased in the Arc by 2-Hz EA, but not 100-Hz EA (Guo et al., 1996). Also, lesions of the Arc almost completely blocked 2-Hz EA analgesia but did not affect

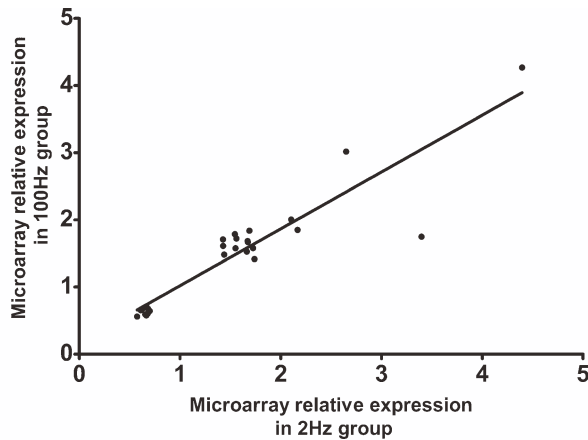


Fig. 3. Scatterplot of coregulated genes/ESTs by 2-Hz and 100-Hz EA. Gene expression regulation was determined with the microarray data and compared with reference samples from the control group. Coregulated genes/ESTs by 2-Hz and 100-Hz EA were changed in the same direction (Pearson's correlation coefficient,  $R = 0.92$ ,  $P < 0.001$ ).

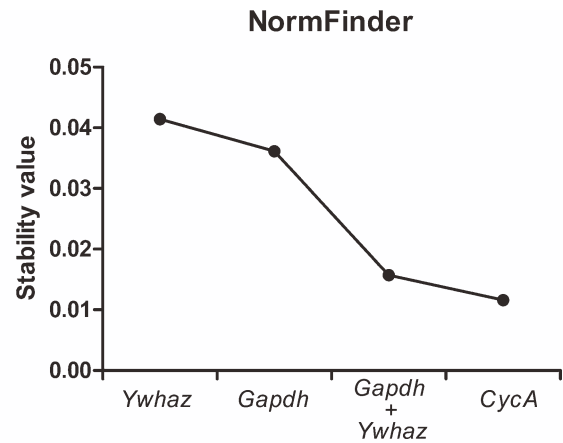


Fig. 4. Gene stability according to NormFinder software. *CycA* was the most stable gene, with the lowest stability values.

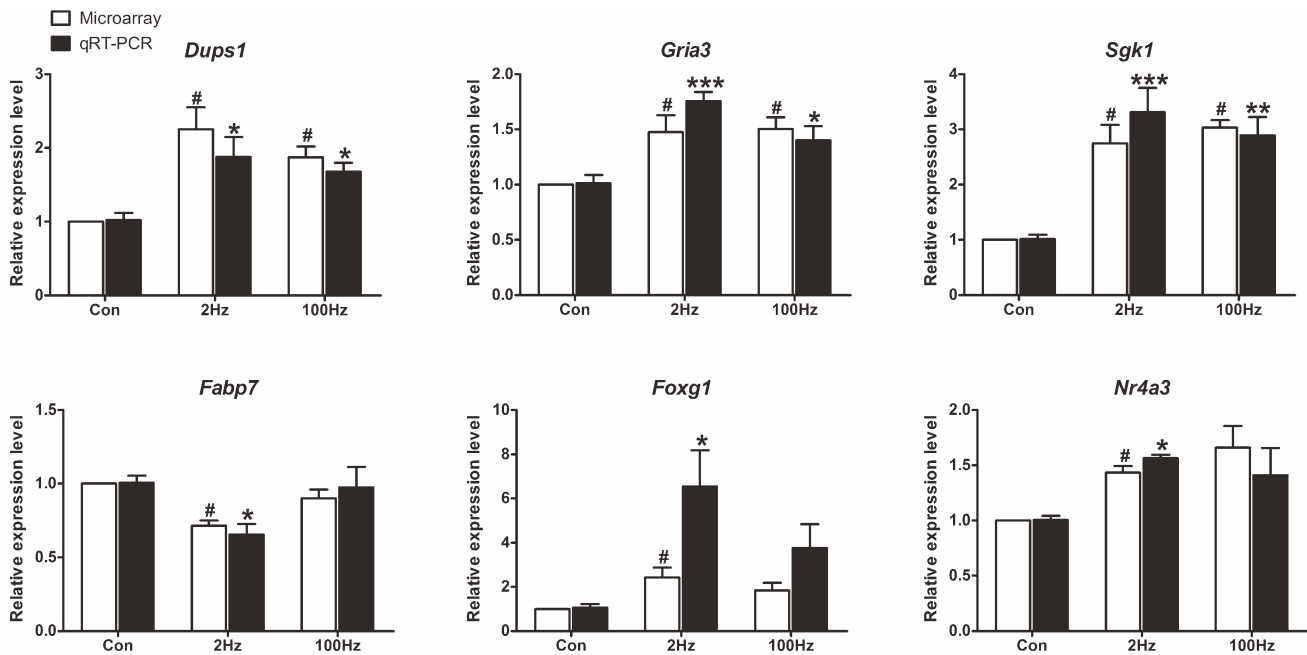


Fig. 5. qRT-PCR confirmation of differentially regulated genes of interest predicted by microarrays. Data are expressed as mean  $\pm$  SEM. \* $P < 0.05$ , \*\* $P < 0.01$ , and \*\*\* $P < 0.001$  vs. control group in qRT-PCR experiment. #Differentially expressed genes/ESTs identified using SAM analysis in the microarray experiment.

TABLE V. qRT-PCR and DNA Microarray Results\*

Symbol	2-Hz EA		100-Hz EA	
	qRT-PCR fold change <sup>a</sup>	Microarray fold change	qRT-PCR fold change <sup>a</sup>	Microarray fold change
<i>Dups1</i>	2.03 ± 0.33	2.25 ± 0.33	1.75 ± 0.14	1.88 ± 0.16
<i>Gria3</i>	1.79 ± 1.10	1.48 ± 0.16	1.44 ± 0.14	1.50 ± 0.12
<i>Sgk1</i>	2.94 ± 0.32	2.75 ± 0.36	2.88 ± 0.36	3.03 ± 0.15
<i>Fabp7</i>	0.65 ± 0.08	0.72 ± 0.04	1.02 ± 0.16	0.90 ± 0.06
<i>Foxg1</i>	5.91 ± 1.34	2.42 ± 0.49	2.99 ± 0.93	1.83 ± 0.38
<i>Nr4a3</i>	1.62 ± 0.03	1.43 ± 0.06	1.44 ± 0.28	1.66 ± 0.22

\*Results are expressed as the mean ± SEM.

<sup>a</sup>Fold changes are expressed as the ratio between alcohol-treated and control samples; a ratio higher than 1 represents up- and a ratio lower than 1 represents downregulation of gene expression.

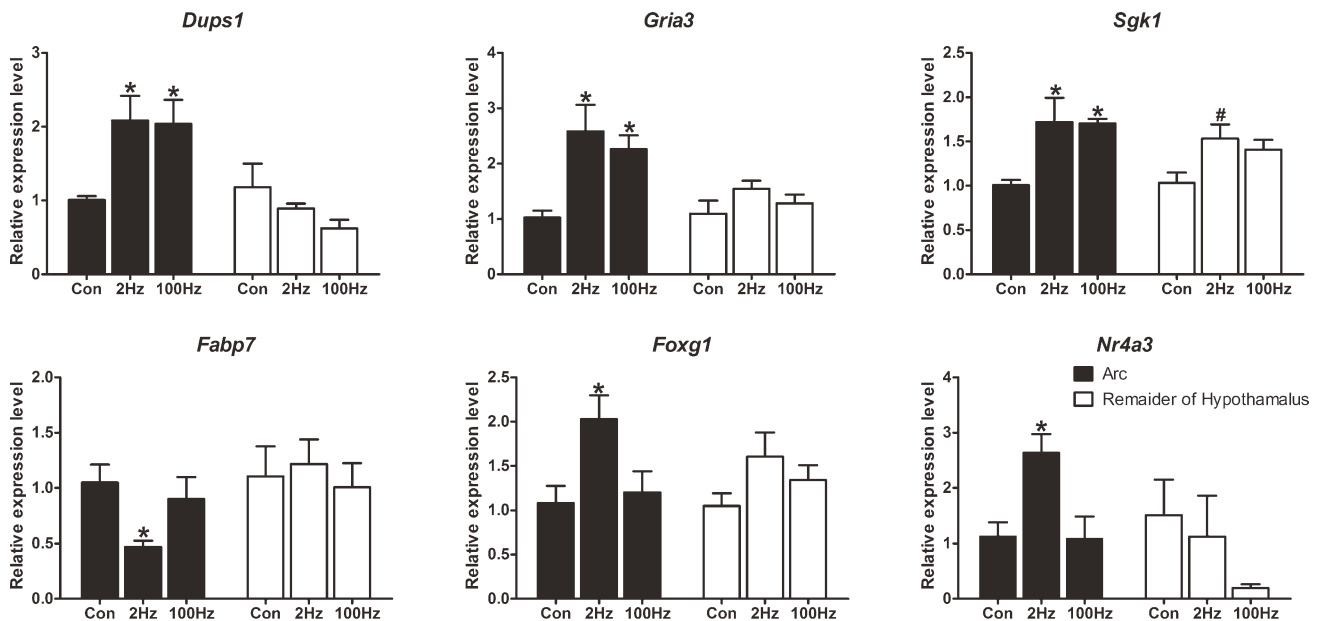


Fig. 6. Region-specifically regulated genes in the Arc region with 2-Hz/100-Hz EA stimuli by qRT-PCR. Data are expressed as mean ± SEM. \* $P < 0.05$  vs. control group in Arc samples. # $P < 0.05$  vs. control group in the remaining hypothalamus around the Arc samples.

100-Hz EA analgesia (Wang et al., 1990; Guo et al., 1996). Other studies also confirmed that Arc was associated with mediating low-frequency EA effects (Take-shige et al., 1992; Guo and Longhurst, 2007, 2010). These results suggested that the EA response is a highly orchestrated, frequency-dependent biological process in different neural regions and that the Arc region mainly responded to 2-Hz EA stimuli.

By combining the results of GO annotations and the key regulatory process identified by DAVID analysis, we found that specific GO categories were uniquely enriched by 2-Hz EA stimulation. These enriched GO categories were related to neurogenesis, and their regulated genes were all upregulated. For example, the transcription factor *Foxg1* regulates neurogenesis in a number of neurodevelopmental processes and promotes the survival of postmitotic neurons (Dastidar et al., 2011). *Nr4a3*, a member of the nuclear receptor family of transcription factors, plays a key role in mediating

neuronal differentiation and activity-dependent maintenance of neuronal plasticity (Ponnio and Conneely, 2004). *Zfp423*, as a DNA-binding transcription factor, controls proliferation and differentiation of neural precursors in cerebellar vermis formation (Alcaraz et al., 2006). In this study, *Foxg1*, *Nr4a3*, and *Zfp423* were consistently upregulated by 2-Hz EA treatment. Clinical research indicated that low-frequency EA has a positive effect in motor function recovery after ischemic stroke (Y.S. Kim et al., 2008). Given our results, 2-Hz EA might be a better treatment for nervous system injury by activating a variety of neurogenesis-related genes. In addition, the mRNA expression of *Fabp7* was also upregulated by 2-Hz EA. *Fabp7*, a brain-type fatty acid-binding protein, plays an important role in CNS development. The Arc is a crucial integrative center for modulation of food intake (Cowley et al., 2001). It has been showed that *Fabp7* has an unusually intense immunoreactivity in the Arc region and a potent influence on



the regulation of feeding behavior and energy homeostasis (Young, 2002). In both experimental and clinical applications, 2-Hz EA was effective for reduction of the body weight accompanied by a reduction in food intake (Wang et al., 2008). EA at 2-Hz was more effective than 100-Hz EA (Tian et al., 2005). Given our results, *Fabp7* may be an important regulated gene in Arc in response to the low-frequency EA treatment for obesity.

Pathway-level analysis of -omics data provides an essential means for systems biology to capture the systematic properties of the inner activities of cells. With pathway enrichment analysis, the LTD pathway was significantly regulated by 2-Hz EA stimulation. Three components of LTD were hit: *Plcb1*, *Gria3*, and *Gnas*. LTD in the CNS is a process that may be involved in learning and memory and various physiological and pathological processes in different regions of the CNS (Collingridge et al., 2010). One study also showed that EA at the low frequency of 2 Hz applied to acupoints ST36 and SP6 could induce LTD of the C-fiber-evoked potentials in SNL rats to relieve neuropathic pain effectively and was different from the high frequency of 100 Hz (Xing et al., 2007). In this study, *Plcb1*, *Gria3*, and *Gnas* were upregulated. This indicates that these genes may play important roles in induction of LTD expression by 2-Hz EA. Our previous study showed that Arc in the hypothalamus was a main response region with 2-Hz EA (Wang et al., 1990; Guo et al., 1996). Compared with the remaining tissues of the hypothalamus around the Arc, these regulated genes induced by 2-Hz EA were mainly regulated especially in the Arc region by qRT-PCR (Fig. 6). However, further morphological verification is required to confirm the interesting regulated genes and whether their expression change exists only in the Arc region or also in other regions. Furthermore, physiopathological and behavior tests should be used to exploit these special regulated genes in Arc related to 2-Hz EA effects.

In the 100-Hz group, it was found that the GO category of regulation of apoptosis and the pathway of MAPK signaling pathway were enriched, which were related to neurogenesis. However, three genes (*Sgk1*, *Dusp1* and *Nr4a1*) among the total of five regulated genes by 100-Hz EA in these enriched GO and pathway were also regulated in the 2-Hz group (Supp. Info. Table 4). Moreover, all of the 27 coregulated genes after 2-Hz/100-Hz EA stimulations had similar directions (up or down; Fig. 3), and only one GO category of regulation of apoptosis was enriched (Table IV). Thus, the Arc involvement in the EA response was a common characteristic with different frequencies.

In summary, this research indicates that the gene expression profile of the Arc region could be effectively and specifically regulated by EA with different frequencies. Particularly, the Arc region showed more gene expression with low-frequency EA. Furthermore, the neurogenesis-related genes were widely regulated by EA, especially by 2-Hz stimulation. This may explain why the low-frequency EA was effective in relieving patients' pain caused by neural injury in the clinic.

## REFERENCES

- Alcaraz WA, Gold DA, Raponi E, Gent PM, Concepcion D, Hamilton BA. 2006. Zfp423 controls proliferation and differentiation of neural precursors in cerebellar vermis formation. *Proc Natl Acad Sci U S A* 103:19424–19429.
- Andersen CL, Jensen JL, Orntoft TF. 2004. Normalization of real-time quantitative reverse transcription-PCR data: a model-based variance estimation approach to identify genes suited for normalization, applied to bladder and colon cancer data sets. *Cancer Res* 64:5245–5250.
- Bonefeld BE, Elfving B, Wegener G. 2008. Reference genes for normalization: a study of rat brain tissue. *Synapse* 62:302–309.
- Bustin SA, Benes V, Garson JA, Hellemans J, Huggett J, Kubista M, Mueller R, Nolan T, Pfaffl MW, Shipley GL, Vandesompele J, Wittwer CT. 2009. The MIQE guidelines: minimum information for publication of quantitative real-time PCR experiments. *Clin Chem* 55:611–622.
- Cassaglia PA, Hermes SM, Aicher SA, Brooks VL. 2011. Insulin acts in the arcuate nucleus to increase lumbar sympathetic nerve activity and baroreflex function in rats. *J Physiol* 589:1643–1662.
- Collingridge GL, Peineau S, Howland JG, Wang YT. 2010. Long-term depression in the CNS. *Nat Rev Neurosci* 11:459–473.
- Cowley MA, Smart JL, Rubinstein M, Cerdan MG, Diano S, Horvath TL, Cone RD, Low MJ. 2001. Leptin activates anorexigenic POMC neurons through a neural network in the arcuate nucleus. *Nature* 411:480–484.
- Dastidar SG, Landrieu PM, D'Mello SR. 2011. FoxG1 promotes the survival of postmitotic neurons. *J Neurosci* 31:402–413.
- Guo HF, Tian J, Wang X, Fang Y, Hou Y, Han J. 1996. Brain substrates activated by electroacupuncture of different frequencies (I): Comparative study on the expression of oncogene c-fos and genes coding for three opioid peptides. *Brain Res Mol Brain Res* 43:157–166.
- Guo ZL, Longhurst JC. 2007. Expression of c-Fos in arcuate nucleus induced by electroacupuncture: relations to neurons containing opioids and glutamate. *Brain Res* 1166:65–76.
- Guo ZL, Longhurst JC. 2010. Activation of reciprocal pathways between arcuate nucleus and ventrolateral periaqueductal gray during electroacupuncture: involvement of VGLUT3. *Brain Res* 1360:77–88.
- Han JS. 2003. Acupuncture: neuropeptide release produced by electrical stimulation of different frequencies. *Trends Neurosci* 26:17–22.
- Han JS. 2011. Acupuncture analgesia: areas of consensus and controversy. *Pain* 152:S41–S48.
- Huang da W, Sherman BT, Lempicki RA. 2009. Systematic and integrative analysis of large gene lists using DAVID bioinformatics resources. *Nat Protoc* 4:44–57.
- Hui KK, Liu J, Marina O, Napadow V, Haselgrove C, Kwong KK, Kennedy DN, Makris N. 2005. The integrated response of the human cerebro-cerebellar and limbic systems to acupuncture stimulation at ST 36 as evidenced by fMRI. *Neuroimage* 27:479–496.
- Kim HW, Uh DK, Yoon SY, Roh DH, Kwon YB, Han HJ, Lee HJ, Beitz AJ, Lee JH. 2008. Low-frequency electroacupuncture suppresses carrageenan-induced paw inflammation in mice via sympathetic post-ganglionic neurons, while high-frequency EA suppression is mediated by the sympathoadrenal medullary axis. *Brain Res Bull* 75:698–705.
- Kim YS, Hong JW, Na BJ, Park SU, Jung WS, Moon SK, Park JM, Ko CN, Cho KH, Bae HS. 2008. The effect of low vs. high frequency electrical acupoint stimulation on motor recovery after ischemic stroke by motor evoked potentials study. *Am J Chin Med* 36:45–54.
- Li AH, Zhang JM, Xie YK. 2004. Human acupuncture points mapped in rats are associated with excitable muscle/skin-nerve complexes with enriched nerve endings. *Brain Res* 1012:154–159.
- Li HY, Zhang R, Cui CL, Han JS, Wu LZ. 2011. Damage of splenic T lymphocyte proliferation and differentiation and its normalization by electroacupuncture in morphine-dependent mice mode. *Evid Based Complement Alternat Med* 2011:424092.

- Liu J, Garza JC, Truong HV, Henschel J, Zhang W, Lu XY. 2007. The melanocortinergic pathway is rapidly recruited by emotional stress and contributes to stress-induced anorexia and anxiety-like behavior. *Endocrinology* 148:5531–5540.
- Paxinos G, Watson C. 1998. *The rat brain in stereotaxic coordinates*. San Diego: Academic.
- Peng JM, Xu LS, Zhu Q, Gong S, Yu XM, Guo SY, Wu GC, Tao J, Jiang XH. 2011. Enhanced NMDA receptor NR1 phosphorylation and neuronal activity in the arcuate nucleus of hypothalamus following peripheral inflammation. *Acta Pharmacol Sin* 32:160–166.
- Ponnio T, Conneely OM. 2004. *nor-1* Regulates hippocampal axon guidance, pyramidal cell survival, and seizure susceptibility. *Mol Cell Biol* 24:9070–9078.
- Rho SW, Choi GS, Ko EJ, Kim SK, Lee YS, Lee HJ, Hong MC, Shin MK, Min BI, Kee HJ, Lee CK, Bae HS. 2008. Molecular changes in remote tissues induced by electro-acupuncture stimulation at acupoint ST36. *Mol Cells* 25:178–183.
- Robinson GE. 2004. Genomics. Beyond nature and nurture. *Science* 304:397–399.
- Senna-Fernandes V, Franca DL, de Souza D, Santos KC, Sousa RS, Manoel CV, Santos-Filho SD, Bernardo-Filho M, Guimaraes MA. 2009. Acupuncture at “zusanli” (St.36) and “sanyinjiao” (SP.6) points on the gastrointestinal tract: a study of the bioavailability of <sup>99m</sup>Tc-sodium pertechnetate in rats. *Evid Based Complement Alternat Med* [PMID 19213853].
- Takehige C, Sato T, Mera T, Hisamitsu T, Fang J. 1992. Descending pain inhibitory system involved in acupuncture analgesia. *Brain Res Bull* 29:617–634.
- Tian DR, Li XD, Wang F, Niu DB, He QH, Li YS, Chang JK, Yang J, Han JS. 2005. Upregulation of the expression of cocaine and amphetamine-regulated transcript peptide by electroacupuncture in the arcuate nucleus of diet-induced obese rats. *Neurosci Lett* 383:17–21.
- Tusher VG, Tibshirani R, Chu G. 2001. Significance analysis of microarrays applied to the ionizing radiation response. *Proc Natl Acad Sci U S A* 98:5116–5121.
- Ulett GA, Han S, Han JS. 1998. Electroacupuncture: mechanisms and clinical application. *Biol Psychiatry* 44:129–138.
- Wang F, Tian DR, Han JS. 2008. Electroacupuncture in the treatment of obesity. *Neurochem Res* 33:2023–2027.
- Wang H, Pan Y, Xue B, Wang X, Zhao F, Jia J, Liang X. 2011. The antioxidative effect of electro-acupuncture in a mouse model of Parkinson’s disease. *PLoS One* 6:e19790.
- Wang JZ, Zhou HJ, Liu GL, Yuan Y, Yan SC, Luo F, Chen XH, Han JS. 2000. Post-traumatic spasticity treated with Han’s acupoint nerve stimulator (HANS). *Chin J Pain Med* 6:217–224.
- Wang K, Xiang XH, He F, Lin LB, Zhang R, Ping XJ, Han JS, Guo N, Zhang QH, Cui CL, Zhao GP. 2010. Transcriptome profiling analysis reveals region-distinctive changes of gene expression in the CNS in response to different moderate restraint stress. *J Neurochem* 113:1436–1446.
- Wang Q, Mao L, Han J. 1990. The arcuate nucleus of hypothalamus mediates low but not high frequency electroacupuncture analgesia in rats. *Brain Res* 513:60–66.
- Xie ZQ, Liang G, Zhang L, Wang Q, Qu Y, Gao Y, Lin LB, Ye S, Zhang J, Wang H, Zhao GP, Zhang QH. 2009. Molecular mechanisms underlying the cholesterol-lowering effect of *Ginkgo biloba* extract in hepatocytes: a comparative study with lovastatin. *Acta Pharmacol Sin* 30:1262–1275.
- Xing GG, Liu FY, Qu XX, Han JS, Wan Y. 2007. Long-term synaptic plasticity in the spinal dorsal horn and its modulation by electroacupuncture in rats with neuropathic pain. *Exp Neurol* 208:323–332.
- Young JK. 2002. Anatomical relationship between specialized astrocytes and leptin-sensitive neurones. *J Anat* 201:85–90.
- Zhang JL, Zhang SP, Zhang HQ. 2009. Effect of electroacupuncture on thalamic neuronal response to visceral nociception. *Eur J Pain* 13:366–372.
- Zhao ZQ. 2008. Neural mechanism underlying acupuncture analgesia. *Prog Neurobiol* 85:355–375.
- Zou R, Zhang HX, Zhang TF. 2006. Comparative study on treatment of acute gouty arthritis by electroacupuncture with different frequency. *Chin J Integr Med* 12:212–214.